Analysis of Crack Development, Both Growth and Closure, in Steel Oxide Scale Under Hot Compression

Michal Krzyzanowski, Piyada Suwanpinij and John H. Beynon

Institute for Microstructural and Mechanical Process Engineering (IMMPETUS), The University of Sheffield, Department of Engineering Materials, Hadfield Building, Mappin Street, Sheffield S1 3JD, UK

Abstract. Numerical analysis based on the finite element method allowed evaluation of conditions for crack development in oxide scale during compression in hot metal forming, particularly in the hot rolling of steel. In addition to cracks formed ahead of contact with the roll, through-thickness cracks can also occur under roll pressure within the roll gap. The modeling has revealed that sometimes cracking that started at the uppermost oxide scale layer was stopped at the thin oxide scale layer nearest to the stock surface. Alternatively, crack closure within the roll gap was possible at high temperature in places where both viscous sliding and ductile behavior of the scale were more pronounced. Many aspects of the modeling are supported by experimental observations.

INTRODUCTION

The important role of the oxide scale in hot metal forming arises from its inevitable position on the interface between tool and workpiece. The secondary oxide scale, growing significantly fast after primary descaling operation, can deform or fracture during metal forming operations. This affects heat transfer and friction during the operation, as well as the quality of the formed product [1, 2]. In hot rolling, for instance, the strain imposed on the strip surface at entry into the roll gap produces longitudinal tensile stresses due to drawing in by frictional contact with the roll. Additionally, bending developed at the roll bite contributes to the stress development. This kind of stress can result in oxide scale failure at the area around the entry zone that has been analyzed numerically using an oxide scale model developed earlier and verified experimentally [3]. It has been shown that the temperature, other rolling parameters, the oxide scale thickness and morphology have significant impact on the failure process. It can result in through-thickness cracking, delamination and spallation of the oxide scale from the strip surface and even transfer of the spalled scale fragments onto the roll surface. The fractured scale can enable direct contact of hot metal with the cold tool due to extrusion of the hot metal through the fractured scale up to the relatively cool roll surface. At higher temperatures the oxide/metal interface can be weaker than the scale itself, and there were indications that some sliding of the oxide scale raft is possible in such conditions. The location of the plane of sliding is determined by the cohesive strength at the different interfaces formed by the metal and the scale sub-layers. Both the fracture and sliding, as well the metal extrusion will produce changes in heat transfer, friction and later after the rolling in quality of the rolled product.

Thus, in the most cases the scale enters the roll gap not as a continuous layer but as a fragmentized layer having relatively small or large through-thickness gaps formed at the entry zone. The scale pattern within the roll gap undergoes further development under the high roll pressure. It is the purpose of this paper to analyse the crack development in the steel oxide scale under the compression at high temperatures, by modelling the scale behaviour using a physically based oxide scale model and applying different experimental techniques to verify the modelling results.

PHYSICALLY BASED MODEL

A physically based oxide scale model allowing for detailed numerical analysis of the micro events at the

CP712, *Materials Processing and Design: Modeling, Simulation and Applications,* NUMIFORM 2004,
edited by S. Ghosh, J. C. Castro, and J. K. Lee

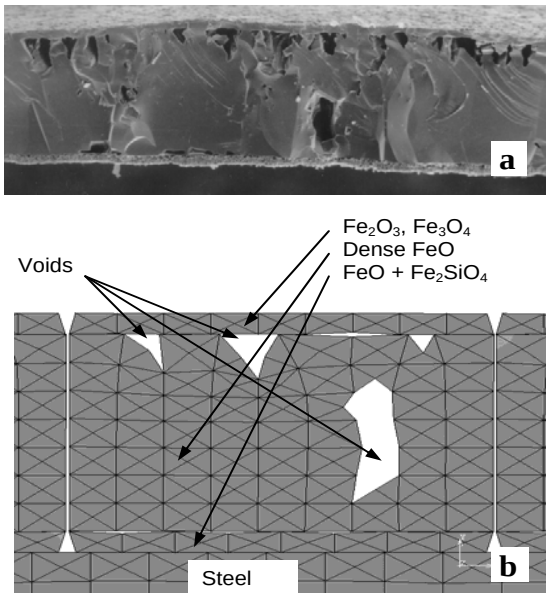

FIGURE 1. SEM image (a) and details of FE mesh (b) representing the cross section of the three-lavers steel oxide scale.

roll gap using the finite element (FE) technique is a central aspect of applied approach. The model is generic, developed gradually by a closely linked combination of laboratory testing and measurements, rolling tests, microstructural investigation coupled with detailed finite element analysis of the observed experimental phenomena [4-6]. The model developed is independent of any particular technological process and represents a numerical approach that can be applied to many metal forming operations, where precise prediction of oxide scale deformation and failure plays a crucial role. The microscopic observations using SEM, BEI, EBSD analysis allows for configuration of the FE model precisely reflecting characteristic morphological features, such as different oxide sub-layers, voids, roughness of the interfaces, ratio between the layers for different temperatures, oxidation times and steel composition (Fig. 1). Adjustment of the model, which is usually a micro-part of the complex FE model, for a particular configuration is necessary stage for prediction of a desired technological parameter.

The separation loads within the oxide scale and at the scale/metal interface measured during modified hot tensile testing are the most critical parameters for scale failure [7]. They depend on the morphology of the particular oxide scale, scale growth temperature and are also very sensitive to the chemical composition of the underlying steel. Application of the model to provide numerical analysis of experimental results significantly improves accuracy in determining these relatively small loads. Matching the predicted and measured loads at the end of the specimen allows for determination of the strain energy release rate that is a critical parameter for prediction of crack propagation within the scale or along the scale/metal interface. The method has been developed for steel oxides, which show both brittle failure at low temperature range (usually less than 800^{o}C) and ductile fracture at high temperatures. The critical strain for failure is implemented into the model for the first case, while for the case of ductile behaviour the J-integral is used as a parameter corresponding to the strain energy release rate during scale failure. It has been assumed no singularity modelling near the crack tip with a quarter-point node technique and only one contour for the J-integral specified for each interface. In the virtual crack extension method only derivatives of elements of the inverse Jacobian J^{-1} and of the determinant of the Jacobian [J] are invoved:

$$\delta W^e = \int_{V^0} \left(W \delta |J| + \sigma_{ij} \delta J^{-1}_{jk} \frac{\partial u_i}{\partial \eta_k} [J] \right) dV^0 \quad (1)$$

This method, comprehensively described elsewhere [8], appeared to be easier to apply for simulation of crack propagation along the interfaces. The MARC 2000 commercial finite element code was used to simulate metal/scale flow, heat transfer, viscous sliding and failure of the oxide scale during hot rolling assuming the plane strain condition. Releasing nodes were organized using user subroutines in such way that the crack length is determined based on the increment number, then based on the crack length the boundary conditions are deactivated by calling a routine for a specific node number.

MODELLING RESULTS

Figure 2 illustrates the gap patterns typically formed in the oxide scale at entry into the roll gap and at the exit zone. The gaps have different lengths because of the different origin. Some relatively big gaps formed from through-thickness cracks developed at the entry zone due to longitudinal tensile strain in the area. Others, usually small gaps, formed due to bending at the roll bite. The small gaps can become even narrower during passage through the roll gap. They are not filled with metal during the rolling pass while the big gaps can be filled with extruded hot metal, sometimes enabling direct contact with the roll

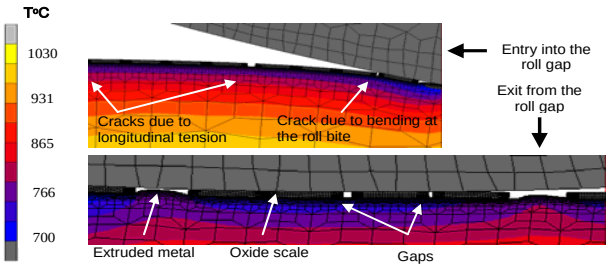

FUGURE 2. Temperature and crack distribution at the oxidized stock/roll interface during hot rolling

surface. The width of the gap between scale fragments is changed under compression because of sliding and deformation of the oxide scale and metal extrusion through the gap. Results of hot compression test modelling have revealed that the sizes of the final gaps depend on many parameters, the first being the initial gap width before the compression (Fig. 3). The initial temperature was 1000°C while the initial scale thickness was 100µm. The cracks with initial widths smaller than 135µm were closed when reduction reached 15% while those initially wider then 200µm were increased. The cracks having an initial width between these critical values remained unchanged or slightly decreased in width. The change in crack width during reduction can be explained by sliding along the metal surface at high temperatures when the scale/metal interface is relatively weak [4]. At the low temperature range, when the interface for this steel is strong enough to sustain the shear stresses influenced by the reduction, the crack width is changed to a less extent, mainly due to deformation. As can be seen (Fig. 4), the scales initially having both the same thickness, 100µm, and the same initial gap width, exhibited different behaviour during compression showing no tendency to be closed at the temperature of

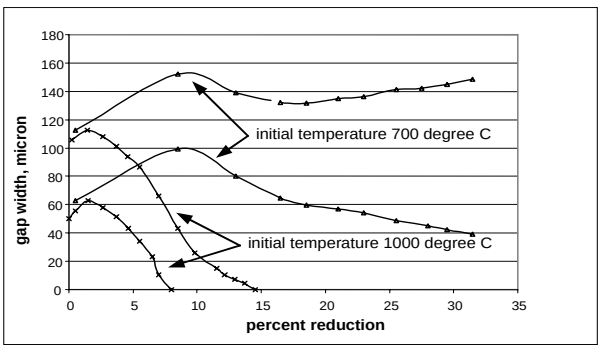

FIGURE 4. Change of the gap in the oxide scale during compression predicted for the different initial temperature

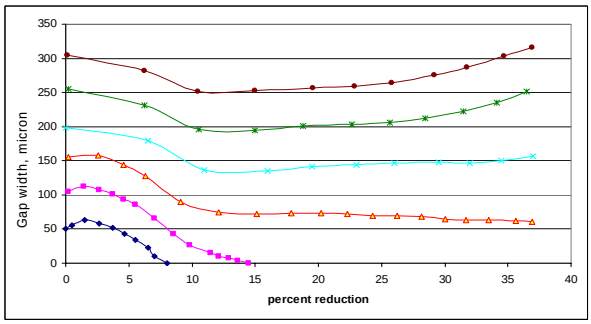

FIGURE 3. Change of the gap in the oxide scale during compression predicted for the different initial gap width

700°C. It can be assumed that there are two critical initial gaps for the oxide scale at the high temperature range. The first one is the critical gap width below which the gap can be closed. The second one is the width above which the gap is increased during compression. Between these critical values, the gap becomes smaller than the initial size (Fig. 5). These opposite tendencies for the scale gap closure and opening during compression can be explained by the tangential loads arising from the compressed metal extruded up to the roll surface at the both edges of the scale fragment. They are more pronounced at higher temperatures. At the low temperature range, the scale/metal interface is stronger and produces shear loads of opposite sign that makes sliding of the scale raft more difficult. Increasing the compression strain rate resulted in closure of the small gaps at higher reduction. The results also exhibited an absence of the second critical width, above which the gap is increased under the compression with the higher strain rate. Tangential viscous sliding of the oxide scale on the

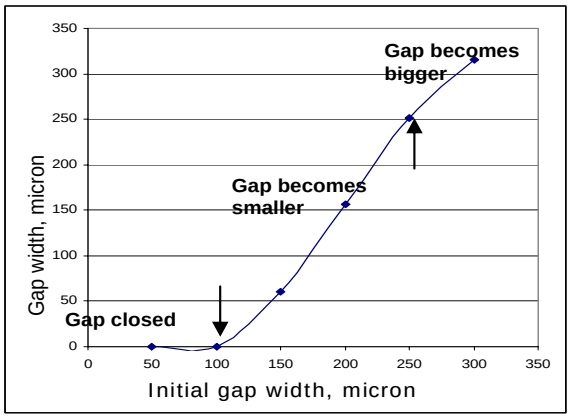

FIGURE 5. Predicted relationship between initial and final gap in the oxide scale during compression

metal surface arising from the shear stress transmitted from the specimen to the scale was allowed in the model. This was assumed in an analogous manner to grain-boundary sliding in high-temperature creep [9]

$$\tau = \eta \, v_{rel} \tag{2}$$

where η is a viscosity coefficient and v_{rel} is the relative velocity between the scale and the metal surface. The viscous sliding of the scale is modelled using a shear-based model of friction such that

$$\eta \, v_{rel} = -m \, k_Y \frac{2}{\pi} \arctan\left(\frac{v_{rel}}{c}\right) \bar{t} \tag{3}$$

where m is the friction factor; k_Y is the shear yield stress; c is a constant taken be 1% of a typical v_{rel} which smoothes the discontinuty in the value of τ when stick/slip transfer occurs; and $\bar{t}$ is the tangent unit vector in the direction of the relative sliding velocity. The calculation of the coefficient η was based on a microscopic model for stress-directed diffusion around irregularities at the interface and depends on the temperature T, the volume-diffusion coefficient D_V, the diffusion coefficient for metal atoms along the oxide/metal interface $\delta_S D_S$ and the interface roughness parameters p and λ [10]

$$\eta = \frac{k \, T \, p^4}{4 \Omega \lambda^2 (\delta_S D_S + 0.8 \, p \, D_V)} \tag{4}$$

where k is Boltzmann's constant, Ω is the atomic volume, $p/2$ is the amplitude and λ is wavelength. It was assumed for the calculation that the diffusion coefficient along the interface was equal to the free surface diffusion coefficient. It can explain the results observed in the modeling that higher strain rates make the viscous sliding more difficult.

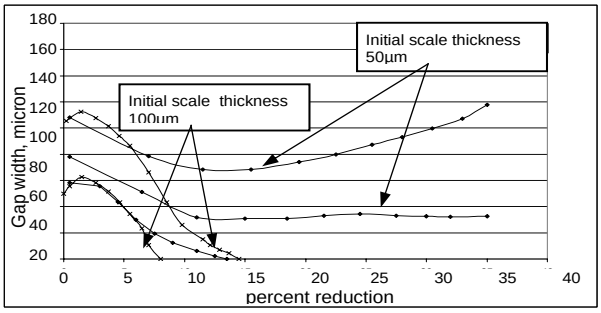

FIGURE 6. Change of the gap in the oxide scale during compression predicted for the different initial scale thickness. Temperature 1000°C.

The thicker oxide scale has shown gap closure at a higher initial gap than the thinner one (Fig. 6). It supports the assumption that the tangential loads arising from compressed metal extruded up to the roll surface at the both edges of the scale fragment initiate sliding of the scale along the interface. The thin scale exhibited a lower tendency to be closed due to the sliding. Shorter scale rafts have shown a better ability to slide under the deformation. This is illustrated in Fig. 7. Before compression both scale rafts had the same initial gap width, 200μm, the initial temperature, 1000°C, and the initial scale thickness, 100μm. At 35% reduction, the gap width became four times shorter than the initial size for the shorter scale rafts while the longer scales allowed for significant metal extrusion through the gap, resulting in its widening which starts at 15% reduction.

It can be noted that the crack development at entry and within the roll gap seems to be more complicated when the oxide scale consists of different sub-layers. Preliminary modelling results obtained for the three layers scale have shown a significant temperature gradient at the oxide scale cross section, that changed the condition for crack development. The cracks did not occur in a through-thickness manner as during one layer scale modelling when the scale temperature was both within the low temperature range and was uniform across the scale thickness. The crack propagation was stopped at thin oxide scale layer situated near the metal surface. This scale layer kept its continuity and adhered to the metal surface while the upper brittle layers were cracked through their thickness [11]. More work should be done to understand their behaviour during compression.

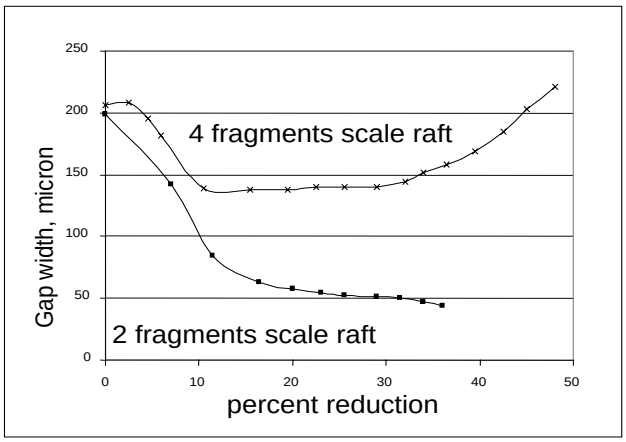

FIGURE 7. Change of the gap in the oxide scale during compression predicted for the different scale length.

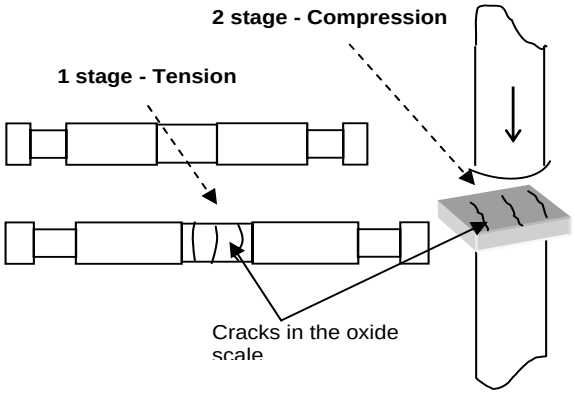

FIGURE 8. Schematic representation of the tesile-compression test

EXPERIMENTAL VERIFICATION

The experimental procedure included two stages, tensile and compression tests, as shown in Fig. 8. The through-thickness cracks were produced in the oxidised flat section of the specimen during the tensile stage. This section was then subjected to uni-axial compression during the second stage. The low carbon steel specimens were oxidised directly in the testing rig using an induction heating system. The oxide scale thickness was about 100µm.

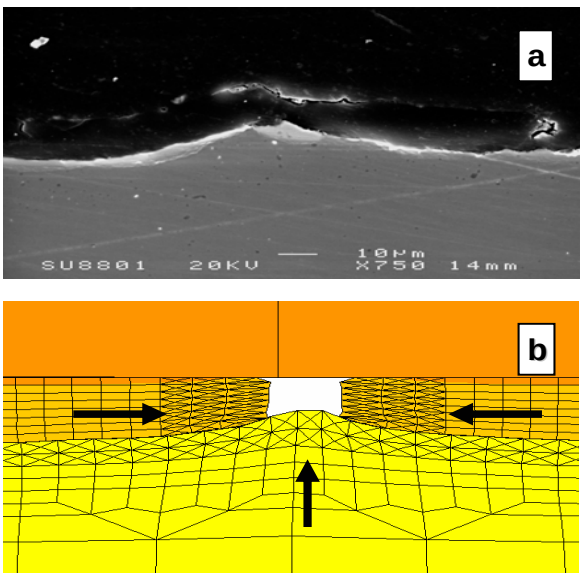

FIGURE 10. SEM photograph of the cross section of the compressed specimen (a) and the results of FEM prediction illustrating formation of the surface profile during compression and closure of the gap.

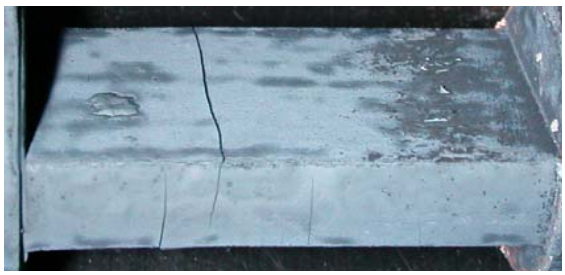

FIGURE 9. State of the specimen after the tensile test. Note the through-thickness crack formed in the oxide scale due to longitudinal tension.

Figure 9 illustrates the crack formed in the oxide scale under 1.5% tensile strain and $0.01s^{-1}$ strain rate at $800^{o}C$. The crack width was 110µm while the scale thickness was about 100µm. The small strain (1.5 – 2%) applied in the tension stage produced relatively narrow through-thickness cracks and prevented spallation of the oxide scale layer. The crack width was measured using optical microscopy while scale morphology was observed using scanning electron microscopy (SEM) after the compression stage. The compression testing was carried out in the high temperature range at which the metal/oxide interface would be relatively weak, enabling possible scale sliding. After the compression test, the specimens were mounted in viscous resin then prepared for SEM analysis performed using Jeol 6400 microscope.

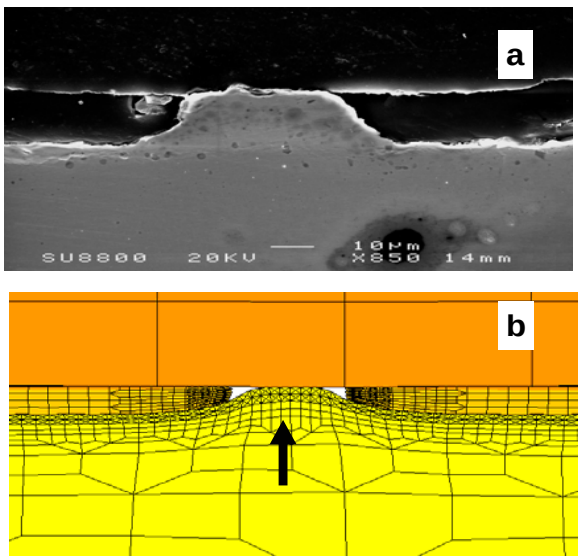

FIGURE 11. SEM photograph of the cross section of the compressed specimen (a) and the results of FEM prediction illustrating formation of the surface profile during compression and metal extrusion through the gap.

Morphologically the oxide scale was inhomogeneous clearly showing two oxide layers. The layer closest to the metal surface consisted of relatively small grains and voids. The outer oxide scale layer exhibited large grains, probably dense FeO, free from big voids and porosity. There were many patches where this outer layer was delaminated or spalled from the rest of the scale. The SEM image shown in Fig 10a illustrates a cross section of the oxide scale after compression at 1000°C. A clearly visible hump, resulting from metal extrusion through the gap formed within the oxide scale during the tensile stage, can be seen at the scale/metal interface. It has to be noted that it is only part of the oxide scale left on the metal surface. The outer part of the scale was spalled after the compression and was transferred to the surface of the upper part of the compression tool. The results indicate the following mechanism for the surface profile formation. The gap width, 110µm, formed after the tension phase, is below the critical width for 100µm thickness oxide scale. The modelling results indicate that for a reduction of more than 20% the profile of the interface should be similar to that shown in Fig. 10b. After spallation of the uppermost layer, only the thinnest (10µm) oxide scale layer was adhered to the metal surface. Figure 11a illustrates the cross section of the interface where the upper part of the oxide scale was spalled just before the compression test, leaving a scale layer of about 20µm thickness, having the gap width of about 80µm. According to the modelling results this gap should be filled with extruded metal under the reduction of 38%. Fig. 11b shows satisfactory agreement with the experiment.

CONCLUSIONS

Numerical analysis of crack development during hot compression of the oxidized low carbon steel was made using the physically based finite element model followed by experimental verification. It has shown that the pre-existing gap between scale fragments is changed under compression because of sliding and deformation of the oxide scale and metal extrusion through the gap. Crack closure eliminates or reduces the metal extrusion and improves the product surface finish. The factors influencing the degree of metal extrusion are the follows:

- the temperature; the scale slides at high temperatures making the initial gap smaller or closed;
- the initial width of the gap; there are two critical initial gaps, the first one is the critical gap width below which the gap can be closed at high temperature. The second one is the gap width above which the gap width is increased. Between these critical values, the gap becomes slightly smaller than the initial one;
- the thickness of the scale; the thicker the oxide scale the larger both critical initial gaps;
- the length of the scale raft; the shorter the fragment of the oxide scale the easier is its ability to slide;
- the strain rate; increase of the strain rate results in closure of the small gaps at higher reduction.

ACKNOWLEDGMENTS

The support from the EPSRC UK (Research Grant GR/R70514/01) is greatly appreciated.

REFERENCES

1. G. Stevens, K. P. Ivens and P. Harper, *J. Iron Steel Inst.* **209**, 1-11 (1971).
2. Y. H. Li and C. M. Sellars, "Modelling deformation behaviour of oxide scales and their effect on interfacial heat transfer and friction during hot rolling" in *Modelling of Metal Rolling Processes,* edited by J.H. Beynon et al., 2nd Int. Conf. Proceedings, The Institute of Materials, London, 1996, pp. 192-206.
3. M. Krzyzanowski, J. H. Beynon and C. M. Sellars, *Metallurgical and Materials Transactions* **31B,** 1483-1490 (2000).
4. M. Krzyzanowski and J. H. Beynon, *Mat. Sci. Techn.* **15,** 1191-1198 (1999).
5. M. Krzyzanowski and J. H. Beynon, *Modelling and Simulation in Materials Science and Engineering* **8,** 927-945 (2000).
6. M. Krzyzanowski, W. Yang, C. M. Sellars and J. H. Beynon, *Mat. Sci. Techn.* **19,** 109-116 (2003).
7. M. Krzyzanowski and J. H. Beynon, *J. Mat. Proc. Techn.* **125-126,** 398-404 (2002).
8. A. Bakker, *Int. J. Pres. Ves. & Piping,* **C14,** 153-179 (1983).
9. H. Riedel, *Metal Science* **16,** 569-574 (1982).
10. R. Raj and M. F. Ashby, *Metall. Trans.* **2A**, 1113-1122 (1971).
11. M. Krzyzanowski, M. Trull and J. H. Beynon, „Numerical identification of oxide scale behaviour under deformation" in *EUROMECH 435*, edited by J. Oudin et al., the FWMF colloquium, Université de Valenciennes, Valenciennes, France, 2002, pp. 95-102.

P.